

## Updated $S$ factors for the ${}^7\text{Be}(p,\gamma){}^8\text{B}$ reaction

A. R. Junghans\*

*Forschungszentrum Dresden Rossendorf, Postfach 510119, D-01324 Dresden, Germany*K. A. Snover,<sup>†</sup> E. C. Mohrmann,<sup>‡</sup> and E. G. Adelberger*Center for Experimental Nuclear Physics and Astrophysics, University of Washington, Seattle, Washington 98195, USA*

L. Buchmann

*TRIUMF, 4004 Wesbrook Mall, Vancouver, British Columbia V6T 2A3, Canada*

(Received 16 September 2009; revised manuscript received 17 December 2009; published 8 January 2010)

We present revised  ${}^7\text{Be}(p,\gamma){}^8\text{B}$   $S$  factors based on our previously published measurements, using a more detailed target analysis and improved stopping powers. Extrapolating our data below the  $1^+$  resonance to solar energies using the latest cluster model calculations of Descouvemont, we find that  $S_{17}(0) = 21.5 \pm 0.6(\text{expt}) \pm 0.7(\text{theor})$  eV b. Fitting all modern, low-energy ( $p, \gamma$ ) data with the same theory, we find a “best” value of  $S_{17}(0) = 20.9 \pm 0.6(\text{expt}) \pm 0.7(\text{theor})$  eV b.

DOI: [10.1103/PhysRevC.81.012801](https://doi.org/10.1103/PhysRevC.81.012801)

PACS number(s): 26.20.-f, 26.65.+t, 25.40.Lw

This Rapid Communication presents a reanalysis of our previously published  ${}^7\text{Be}(p,\gamma){}^8\text{B}$  experimental results [1,2] that incorporates several improvements. We examine the measured  ${}^7\text{Be}(\alpha,\gamma){}^{11}\text{C}$  narrow-resonance profiles and extract independent information on the target composition. We consider the effects of a target composition that varies with depth, and a target areal density that is nonuniform. We use updated SRIM-2008 [3] tables of energy loss and energy loss uncertainties to compute revised proton energy-loss corrections, and we present a table of revised  $S$  factors and uncertainties. Finally, we extrapolate our low-energy data, and other modern low-energy ( $p, \gamma$ ) data below the  $1^+$  resonance, to solar energies using the latest cluster model calculations of Descouvemont [4].

References [1,2] used measured yield profiles for the narrow,  $\Gamma \ll 1$  keV,  ${}^7\text{Be}(\alpha,\gamma)$  resonance at  $E_\alpha = 1377 \pm 2$  keV to monitor the target integrity over time and to compute proton-energy averaging corrections for determining the  ${}^7\text{Be}(p, \gamma)$  cross sections and  $S$  factors. Here we present a more detailed analysis of the resonance profiles.

As discussed in Ref. [2], the high-energy tails of our resonance profiles fall an order of magnitude more slowly than expected from straggling. In the reasonable approximation that the natural resonance width, beam-energy spread, and straggling can be neglected, the  $(\alpha,\gamma)$  resonance yield  $Y(E_\alpha)$  can be written as

$$Y(E_\alpha) = Nf(E_\alpha)/\epsilon_\alpha(E_\alpha), \quad (1)$$

where  $N$  is a normalization constant that includes the resonance strength and detector efficiency,  $f(E_\alpha)$  is the depth-dependent stoichiometric fraction of  ${}^7\text{Be}$ , and  $\epsilon(E_\alpha)$  is the

average stopping power per target atom. Backscattering measurements indicated that the target consisted predominantly of  ${}^7\text{Be}$  and Mo [1,2]. For such a target, the stopping power is given by

$$\epsilon_\alpha(E_\alpha) = f(E_\alpha)\epsilon_{\alpha\text{Be}}(E_\alpha) + [1 - f(E_\alpha)]\epsilon_{\alpha\text{Mo}}(E_\alpha), \quad (2)$$

where  $\epsilon_{\alpha\text{Be}}(E_\alpha)$  and  $\epsilon_{\alpha\text{Mo}}(E_\alpha)$  are the elemental  $\alpha$ - ${}^7\text{Be}$  and  $\alpha$ -Mo stopping powers. The normalization constant  $N$  may be determined from

$$\int Y(E_\alpha)dE_\alpha = Nn_{\text{Be}}, \quad (3)$$

where  $n_{\text{Be}}$  is the total number of  ${}^7\text{Be}$  target atoms/cm<sup>2</sup>. Proton-energy-averaging corrections were computed from

$$\bar{\sigma} = \frac{\int_{E_R}^{E_M} \sigma(E_p)Y(E_\alpha)dE_\alpha}{\int_{E_R}^{E_M} Y(E_\alpha)dE_\alpha}, \quad (4)$$

where  $\sigma(E_p)$  is calculated by assuming an  $S$  factor that is constant over the energy loss in the target (see Ref. [2]). The (laboratory) proton energy  $E_p$  is given by

$$E_p = E_b - \int_{E_R}^{E_\alpha} \frac{\epsilon_p(E_p)}{\epsilon_\alpha(E_\alpha)} dE_\alpha, \quad (5)$$

where  $\epsilon_p(E_p)$  is the average proton stopping power per target atom, given by an expression analogous to Eq. (2),  $E_b$  is the proton bombarding energy,  $E_R$  is the  $\alpha$  resonance energy, and  $E_M$  is the upper energy limit of the profile strength distribution. The results of these proton-energy-averaging calculations are used to infer effective energies and  $S$  factors as described in Ref. [2].

SRIM-2000 stopping powers were used in Refs. [1,2]. Here we update our energy-loss calculations using the latest SRIM-2008 stopping powers and uncertainties [3]. The uncertainty in the  $\epsilon_p/\epsilon_\alpha$  ratio is most relevant for our purposes. Ziegler's stopping-power uncertainties (in percent) for  $p + \text{Be}$  (Mo) and  $\alpha + \text{Be}$  (Mo), based on multiparameter fits to data for each of these four cases, are 5.2, (3.2), 6.1, and (4.0), respectively.

\*A.Junghans@fzd.de

<sup>†</sup>snover@u.washington.edu<sup>‡</sup>Permanent address: DigiPen Institute of Technology, Redmond, Washington 98052, USA.

Because the data are mostly independent, we combine these uncertainties as independent quantities, obtaining  $\pm 5\%$  uncertainty on the ratio, which is larger than we assumed previously.

The shapes of the  $(\alpha, \gamma)$  thick-target resonance profiles shown in Fig. 6 of Ref. [2] have conventional plateau and high-energy tail regions, whereas the leading edges varied with time owing to beam damage. The nearly flat plateau regions of profiles 2 and 3 indicate a uniform composition at mid-depths, whereas the peak near the leading edge of profile 1 indicates a higher than average concentration of  $^7\text{Be}$ .

We analyze the profiles under two different assumptions of the target composition, which we label “varying composition” and “varying thickness”. We show that these lead to nearly identical proton-energy-averaging effects and hence  $S$  factors. In the varying composition approach, we use Eq. (1) to extract  $f(E_\alpha)$  at each point on the  $(\alpha, \gamma)$  resonance profile. Hence the shape of the whole profile is determined by the depth-dependent target composition.

Although this is the most sensible approach for the leading edge and plateau regions of the profiles, it is less appropriate for the high-energy-tail region, as it ascribes the high-energy falloff to an increasingly impure target. In fact, the high-energy tails of the BE3 profiles appear very similar to typical thick-target  $(\alpha, \gamma)$  narrow-resonance profiles measured for pure elemental evaporated targets. In those cases, the slowly falling high-energy tails typically arise from target thickness nonuniformities.

Hence we also make a varying thickness analysis in which we analyze the profiles in and below the plateau region as before, whereas for  $E_\alpha > E_{\text{plat}}$  we assume  $f(E_\alpha) = f_{\text{plat}}$ . In this method, the profile falls at high energies because the target area contains a diminishing fraction of  $^7\text{Be}$ -containing regions at large depths.

The proton-energy-averaging calculations in these two approaches, computed using Eqs. (4) and (5), lead to  $S$  factors that differ by less than 0.4% at the lowest bombarding energy, and by smaller amounts at higher energies. The approaches differ because the  $\epsilon_p(E_p)/\epsilon_\alpha(E_\alpha)$  ratio is evaluated with different assumptions about the behavior of  $f(E_\alpha)$  in the tail region. The insensitivity of the ratio to  $f$  accounts for the good agreement between the two approaches. The close agreement in the proton-energy-averaging calculations performed with the two different profile analysis methods supports the idea that reasonable methods of interpreting the resonance profiles should not lead to substantially different proton-energy-averaging results.

We revised our  $^7\text{Be}(p, \gamma)^8\text{B}$   $S$  factors measured with the BE3 target, using new proton-energy-averaging calculations based on the new SRIM stopping powers and the profile calculations just described. We included additional uncertainty on our data points from stoichiometric ratio uncertainty, profile analysis differences, and possible C buildup effects on the measured profiles. The revised BE3 data errors are somewhat larger for the lowest energy points, whereas the higher energy points are changed very little.

We calculated similar corrections for our BE1 target data and found very small changes. This is because the BE1 target was thinner than the BE3 target, and the BE1 data did not extend as low in energy. Our BE2 target data are completely

TABLE I.  $E$  (keV) and  $S_{17}(E)$  and  $\sigma_{\text{sv}}$  (eV b), where  $\sigma_{\text{sv}}$  is the  $1\sigma$  statistical plus varying systematic error. Additional non-common-mode errors of 0.37% and 0.28% apply to each BE3 S and BE3 L data point, respectively, while an additional common-mode error of 2.3% applies to all BE3 points. For BE1, the common-mode (scale factor) error is 2.7%.

$E$	$S_{17}(E)$	$\sigma_{\text{sv}}$	$E$	$S_{17}(E)$	$\sigma_{\text{sv}}$
	<u>BE1</u>			<u>BE2</u>	
185.6	19.7	0.7	875.7	24.5	0.6
221.8	19.5	0.6	1001.6	24.5	0.6
256.8	19.8	0.6	1403.6	27.4	0.7
293.2	20.1	0.6	1579.4	29.3	0.8
294.1	20.7	0.6	1931.0	34.8	1.0
327.8	20.8	0.5	2194.7	43.3	1.3
363.3	20.8	0.5	2458.5	40.6	1.2
407.6	21.1	0.5		<u>BE3</u>	
460.8	21.5	0.5	116.1	20.2	1.1
496.1	22.4	0.5	140.1	18.9	0.8
528.6	23.2	0.8	184.3	19.7	0.7
558.8	25.9	0.8	255.5	19.4	0.5
589.0	35.5	1.0	277.8	19.8	0.5
599.7	45.6	1.4	326.7	19.7	0.4
609.4	57.9	1.7	362.2	20.7	0.5
619.6	88.4	2.2	872.7	24.7	0.6
633.3	105.5	2.2		<u>BE3 S</u>	
639.4	90.9	2.1	184.6	19.9	0.5
649.2	62.0	1.7	220.0	19.4	0.5
658.7	48.4	1.3	255.6	19.6	0.4
679.1	33.8	1.1	277.7	20.2	0.4
699.4	27.4	0.8	326.6	20.8	0.4
750.7	26.0	0.9	362.2	20.3	0.3
820.7	24.3	0.7	871.5	24.6	0.3
876.3	24.7	0.6	999.5	24.9	0.4
876.3	24.4	0.7	1099.9	25.9	0.3
1002.3	24.6	0.6	1200.1	26.7	0.6
1102.8	25.7	0.7	1754.2	31.1	0.8
1203.2	25.8	0.8			

insensitive to the target properties. Our revised BE1 and BE3 target results are shown in Table I along with our previously published BE2 data. Several typographical errors in Table III of Ref. [2] are also corrected here. The revised low-energy BE1 and BE3  $S$  factors are shown in Fig. 1.

In our previous publications, we extrapolated our  $^7\text{Be}(p, \gamma)^8\text{B}$   $S(E)$  data to  $E = 0$  by fitting the scaled theory of Descouvemont and Baye [5] (DB) to our measured  $S(E)$  values for  $E < 425$  keV (where  $E$  is the mean proton center-of-mass energy, denoted by  $\bar{E}_{\text{c.m.}}$  in Ref. [2]). We again include only low-energy data in our extrapolation to minimize theoretical uncertainty (see the following). Fitting our revised BE1 data with the DB theory yields  $S(0) = 22.6 \pm 0.7$  eV b, whereas for the BE3 data and the DB theory, we obtain  $S(0) = 22.1 \pm 0.6$  eV b. These values and errors are the same as determined previously from fitting our published data [6]. The good agreement between the BE1 and BE3 results affords an important check on systematic errors, since the target thicknesses were different, and the absolute normalizations were determined differently.

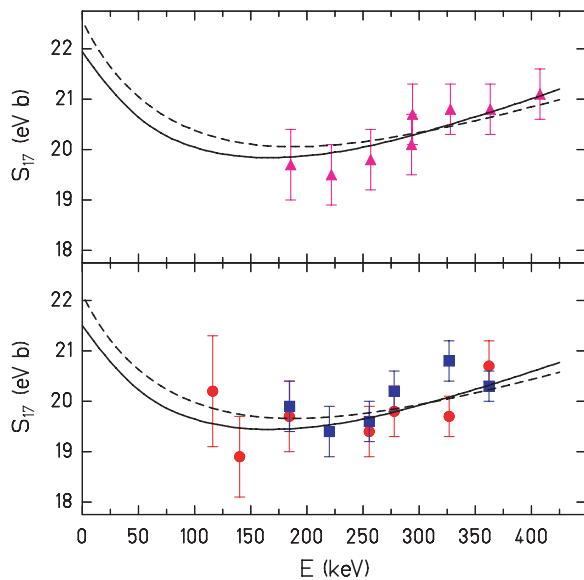


FIG. 1. (Color online) Upper panel: BE1 data. Lower panel: BE3 L (circles); BE3 S (squares). The dashed line represents the DB fit and the solid line represents the D04 fit.

Descouvemont's 2004 cluster-model calculation (D04) improves on the DB calculation by including  ${}^7\text{Be}$  dynamic deformability, the MN nucleon-nucleon interaction, and new experimental information on scattering lengths [4]. The scaled DB and D04 calculations fit our low-energy data equally well, as shown in Fig. 1. Fitting the BE1 and BE3 data with the scaled D04 theory yields  $S(0) = 21.9 \pm 0.6$  and  $21.5 \pm 0.6$  eV b, respectively.

Figure 2 compares the scaled DB and D04 calculations to our data over a wide range, using the  $1^+$  and  $3^+$  resonance components calculated in Ref. [2]. The D04 theory gives a slightly better fit in the the 1–1.5 MeV range, but the improvement relative to DB is minor. Since D04 is an improved theory, we use it for the  $S(0)$  value we recommend from our data:

$$S_{17}(0) = 21.5 \pm 0.6(\text{expt}) \pm 0.7(\text{theor}) \text{ eV b.} \quad (6)$$

Since the BE1 and BE3 experiments have a significant common uncertainty, we do not reduce the error bar on our best  $S(0)$  by averaging. We use the BE3 central value for our “best” value, since we favor somewhat the detector efficiency determination in this experiment.

Our theoretical error is based on Fig. 8 of Ref. [4], which shows that the theoretical extrapolation uncertainty for our fit range is about 3.5%, or 0.7 eV b. This is similar to the 0.6 eV b theoretical uncertainty estimated in Ref. [2] from the distribution of twelve different theories fitted to the Seattle/TRIUMF low-energy data.

Since, to our knowledge, no new  ${}^7\text{Be}(p, \gamma){}^8\text{B}$  experiments have been published since Ref. [2], we analyze the same low-energy data [7–10] that were analyzed in Ref. [2]. We use the D04 theory, and we multiply all fit errors by the inflation factor IF, where  $\text{IF} = \sqrt{\chi^2/\chi^2(P=0.5)}$  whenever  $\chi^2 > \chi^2(P=0.5)$  and unity otherwise [11]. Here  $\chi^2$  is the fit value and  $\chi^2(P=0.5)$  is the  $\chi^2$  corresponding to a probability

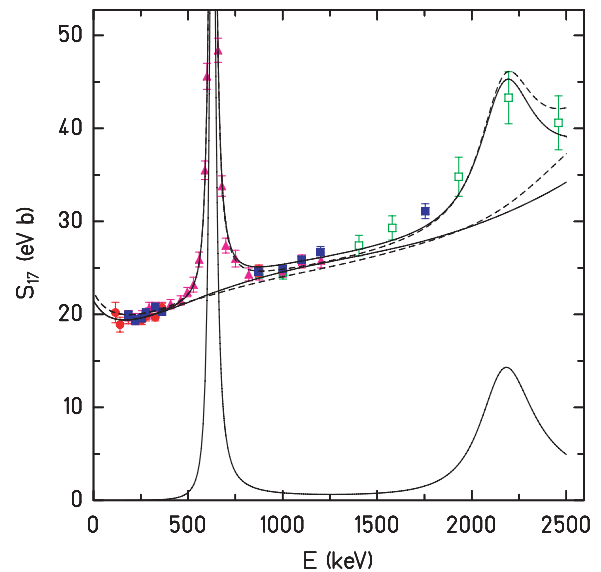


FIG. 2. (Color online) Comparison of scaled DB and D04 calculations with our data: BE3 L (circles), BE3 S (squares), BE1 (triangles), and BE2 (open squares). The upper solid lines are the D04 fit, with and without parametrized  $1^+$  and  $3^+$  resonances. The dashed lines are the DB fit. The lower solid line gives the  $1^+$  and  $3^+$  resonance contributions.

of 50%. Otherwise, we propagate errors as before. The results are shown in Table II. The main effect of these inflation factors is to increase the combined fit error by a factor of 1.22.

As shown in Table II, the combined result from all the modern data with  $E \leq 425$  keV is

$$S_{17}(0) = 20.9 \pm 0.6(\text{expt}) \pm 0.7(\text{theor}) \text{ eV b.} \quad (7)$$

Our previous publications contained several minor errors that we correct here. The  $\alpha$  energies plotted in Fig. 2 of Ref. [1] and Fig. 6 of Ref. [2] are approximately 9 keV too high because, *in these figures only*, an outdated energy calibration was used. On p. 065803-4, the text should read  $t_3 = t_1$ . In Figs. 11–15 of Ref. [2], the S and L symbols are reversed. The slopes quoted in the text on p. 065803-17 are 10 times too large. Other slopes and derived quantities are unchanged. In

TABLE II. Experimental  $S_{17}(0)$  values and uncertainties in eV b and inflation factors (IF) determined by our D04 fits to published data with  $E \leq 425$  keV given in Refs. [7–10]. See Sec. V B of Ref. [2] for additional analysis details.

Experiment	$S_{17}(0)$ (eV b)	Error (eV b)	IF
Filippone	20.1	2.4	1.04
Hammache	19.5	1.4	1.14
Strieder	18.2	1.8	1.07
Baby	20.2	1.3 <sup>a</sup>	1.00
This work	21.5	0.6	1.00
Combined result	20.9	0.6	1.22

<sup>a</sup>To include the target damage error, we use the total error given in the text of Ref. [10], as specified in Ref. [12].

the fits described on p. 065803-17, the  $1^+$  resonance region was excluded in the direct fits, but not in the CD fits.

We have updated our analysis of our published  ${}^7\text{Be}(p,\gamma){}^8\text{B}$  data by making a more detailed analysis of the  ${}^7\text{Be}(\alpha,\gamma){}^{11}\text{C}$  narrow resonance profiles and by using newer stopping powers and errors. We show that the resonance profiles contain important information on the target composition. We analyze the profiles under two different assumptions and show that they lead to nearly identical proton-energy-averaging effects.

DB fits to our revised low-energy BE1 and BE3 data yield the same  $S(0)$  central values and errors as we published

previously. Although  $S(0)$  does not change, the new analysis gives us greater confidence that we understand the  $(\alpha,\gamma)$  narrow-resonance profiles and the effects of finite target thickness. We present new D04 fits to our data and to the other modern data at low energy, and we quote  $S(0)$  values determined from these fits as our best extrapolation to zero energy. Changes in the central value of our recommended  $S_{17}(0)$  are due entirely to improved theory.

We thank M. Gai for comments and for bringing the issue of possible depth-dependent target composition to our attention.

- 
- [1] A. R. Junghans, E. C. Mohrmann, K. A. Snover, T. D. Steiger, E. G. Adelberger, J.-M. Casandjian, H. E. Swanson, L. Buchmann, S. H. Park, and A. Zyuzin, *Phys. Rev. Lett.* **88**, 041101 (2002).
- [2] A. R. Junghans, E. C. Mohrmann, K. A. Snover, T. D. Steiger, E. G. Adelberger, J. M. Casandjian, H. E. Swanson, L. Buchmann, S. H. Park, A. Zyuzin, and A. M. Laird, *Phys. Rev. C* **68**, 065803 (2003).
- [3] [www.srim.org](http://www.srim.org); J. F. Ziegler, *The Stopping and Range of Ions in Matter* (Lulu Press, Morrisville, NC, 2008).
- [4] P. Descouvemont, *Phys. Rev. C* **70**, 065802 (2004).
- [5] P. Descouvemont and D. Baye, *Nucl. Phys.* **A567**, 341 (1994).
- [6] The difference between the 22.6 value quoted here and the 22.3 value given in Ref. [1] is due to the different fit ranges.
- [7] B. W. Filippone, A. J. Elwyn, C. N. Davids, and D. D. Koetke, *Phys. Rev. C* **28**, 2222 (1983). Experimental data were taken from the EXFOR data base at <http://www.nndc.bnl.gov/nndc/exfor>.
- [8] F. Hammache, G. Bogaert, P. Aguer, C. Angulo, S. Barhoumi, L. Brillard, J. F. Chemin, G. Claverie, A. Coc, M. Hussonnois, M. Jacotin, J. Kiener, A. Lefebvre, J. N. Scheurer, J. P. Thibaud, and E. Virassamynäiken, *Phys. Rev. Lett.* **80**, 928 (1998); F. Hammache, Ph.D. thesis (Universite de Paris XI, Orsay, 1999); F. Hammache, G. Bogaert, P. Aguer, C. Angulo, S. Barhoumi, L. Brillard, J. F. Chemin, G. Claverie, A. Coc, M. Hussonnois, M. Jacotin, J. Kiener, A. Lefebvre, J. N. Scheurer, J. P. Thibaud, and E. Virassamynäiken, *Phys. Rev. Lett.* **86**, 3985 (2001).
- [9] F. Strieder, L. Gialanella, G. Gyürky, F. Schümann, R. Bonetti, C. Broggin, L. Campajola, P. Corvisiero, H. Costantini, A. D'Onofrio, A. Formicola, Z. Fülöp, G. Gervino, U. Greife, A. Guglielmetti, C. Gustavino, G. Imbriani, M. Junker, P. G. P. Moroni, A. Ordine, P. Prati, V. Roca, D. Rogalla, C. Rolfs, M. Romano, E. Somorjai, O. Straniero, F. Terrasi, H. P. Trautvetter, and S. Zavatarelli, *Nucl. Phys.* **A696**, 219 (2001); F. Strieder, Ph.D. thesis, Ruhr Universität Bochum, 2000.
- [10] L. T. Baby, C. Bordeanu, G. Goldring, M. Hass, L. Weissman, V. N. Fedoseyev, U. Köster, Y. Nir-El, G. Haquin, H. W. Gäggeler, and R. Weinreich (ISOLDE Collaboration), *Phys. Rev. Lett.* **90**, 022501 (2003); *Phys. Rev. C* **67**, 065805 (2003); **69**, 019902(E) (2004).
- [11] This is the same procedure adopted recently at the Solar Fusion workshop, [http://www.int.washington.edu/PROGRAMS/solar\\_fusion.html](http://www.int.washington.edu/PROGRAMS/solar_fusion.html) (Rev. Mod. Phys., to be published).
- [12] M. Hass (private communication, 2003, 2009).